FULL PAPER

Dalton
www.rsc.org/dalton

Coordination of gadolinium(III) ions with a preformed μ-oxo diiron(III) complex: structural and magnetic data

Jean-Pierre Costes,* Françoise Dahan, Frédéric Dumestre, Juan Modesto Clemente-Juan,† Javier Garcia-Tojal‡ and Jean-Pierre Tuchagues

Laboratoire de Chimie de Coordination du CNRS, UPR 8241, liée par conventions à l'Université Paul Sabatier et à l'Institut National Polytechnique de Toulouse, 205 route de Narbonne, 31077 Toulouse Cedex, France. E-mail: costes@lcc-toulouse.fr

Received 7th November 2002, Accepted 4th December 2002
First published as an Advance Article on the web 14th January 2003

A hexadentate ligand LH_2 (LH_2 = 1,2-bis((3-methoxysalicylidene)amino)ethane) reacts with iron(III) ions to yield a μ-oxo complex $(LFe)_2O$, **1**, which may function as a ligand towards gadolinium(III). The resulting product is a tetranuclear complex $[LFeGd(NO_3)_3]_2O$, **2**. Its structure has been determined by single crystal X-ray crystallography: **2**, monoclinic $P2_1/n$ (No. 14), a = 15.346(2), b = 17.372(2), c = 19.625(2) Å, β = 100.59(1)°, Z = 4. The thermal dependence of the $\chi_M T$ product (χ_M = molar magnetic susceptibility) and the field dependence of the magnetization (M) have been measured and analyzed according to the spin cluster model. In both complexes the Fe–Fe interaction is antiferromagnetic with a magnitude of −115.3 cm^{-1} (**1**) and −101.4 cm^{-1} (**2**). In the latter compound an exchange coupling is operative within each (Fe^{III}, Gd^{III}) pair. Modelling of the experimental data ($\chi_M T$ and M) leads to the conclusion that this interaction is small and, unexpectedly, antiferromagnetic.

Introduction

The present paper is devoted to an unprecedented tetranuclear $(Fe^{III}, Gd^{III})_2$ complex which displays an $S = 0$ spin ground state resulting from (Fe, Fe) and (Fe, Gd) antiferromagnetic interactions. Until recently ferromagnetic interaction was considered as an intrinsic property of the (M, Gd) pairs regardless of their nature and characteristics, M standing for an organic radical,[1–3] or a 3d ion.[4–10] In the past two years a few exceptions to this general trend have been reported. They concern two complexes involving a gadolinium ion and organic radicals[11,12] and six (M, Gd) complexes with M = Cu^{II} or VO^{II}.[13,14] It may be noted that one (Fe^{III}, Gd^{III})[10] and three (Fe^{II}, Gd^{III}) complexes[15] have been described. They show ferromagnetic (3d, 4f) interactions.

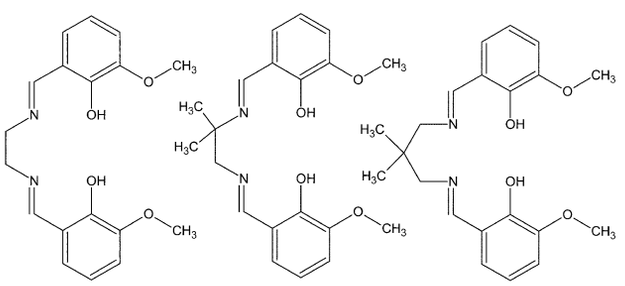

LH_2 S = 2 L^2H_2 S = 1 L^1H_2

Scheme 1 Schematic representation of the Schiff base ligands.

Results and discussion

Preparation and characterization

The LH_2 ligand (LH_2 = 1,2-bis((3-methoxysalicylidene)amino)-ethane) is a hexadentate ligand that possesses two differentiated coordination sites and thus is tailor-made to bind two different metal ions. Methyl substitutions onto the diamino chain lead to a series of ligands (quoted L^SH_2 in the following, Scheme 1) which have allowed the successive isolation of mononuclear ferrous complexes and dinuclear (Fe^{II}, Gd^{III}) species.[15] These complexes are fairly stable under nitrogen atmosphere. At variance with this behaviour, reaction of the ferrous complex of the unsubstituted ligand LH_2 with gadolinium ions yields a mixture which, on the basis of spectroscopic data, contains the starting material LFe^{II} (80%) and surprisingly, a (Fe^{III}, Gd^{III}) species (20%). This prompted us to study the behaviour of the ternary system $Fe^{III}/LH_2/Gd^{III}$. According to the process described in the experimental section we succeeded in isolating successively the dimetallic complex **1** and the tetrametallic complex **2**. Their nature was substantiated by chemical analysis, Mössbauer spectroscopy and structural determination. **1** is a genuine μ-oxo diiron(III) complex and **2** is a tetranuclear species which results from the insertion of a gadolinium ion into each vacant coordination site of the dinuclear ferric complex **1**.

Mössbauer spectra of both complexes (recorded at 180 K) display a quadrupole doublet with an isomer shift δ = 0.334 and 0.289 mm s^{-1} and a quadrupole splitting ΔE_Q = 0.865 and 0.805 mm s^{-1} for **1** and **2**, respectively. The Mössbauer parameters of **1** and **2** are similar and consistent with the presence of ferric ions.[16,17] As expected, they deviate significantly from those obtained for the related ferrous complexes L^1Fe^{II} and L^1Fe^{II}-$Gd^{III}(NO_3)_3$, *i.e.* δ = 1.099 mm s^{-1}, 1.059 mm s^{-1} and ΔE_Q = 2.464 mm s^{-1}, 2.609 mm s^{-1}, respectively.[15] Interestingly, the values characterizing **1** are identical to the parameters of one of the doublets previously observed for the mixture resulting from the reaction of Gd^{III} ions with LFe^{II}. In this respect, one may speculate that LFe^{II} would have a low affinity for the lanthanide ions but could react with residual oxygen and moisture of the solvents and atmosphere to produce some amount of a μ-oxo diferric species which could subsequently react with Gd^{III} ions. Such a differentiated reactivity towards oxygen and 4f ions seems to be closely connected to the nature of the unsubstituted ligand LH_2.

Structural study

The structure of **2** is shown in Fig. 1. A prominent characteristic feature of the structure is the presence of a μ-oxo diiron unit which is a fundamental structural component of iron chemistry.[17–20] The two metal ions adopt a distorted square-based

† Present address: Instituto de Ciencia Molecular, Universidad de Valencia, Dr. Moliner 50, 46100 Burjassot, Spain.
‡ Present address: Dpto de Quimica, Universidad de Burgos, Misael Bañuelos, s/n, 09001 Burgos, Spain.

DOI: 10.1039/b210950f

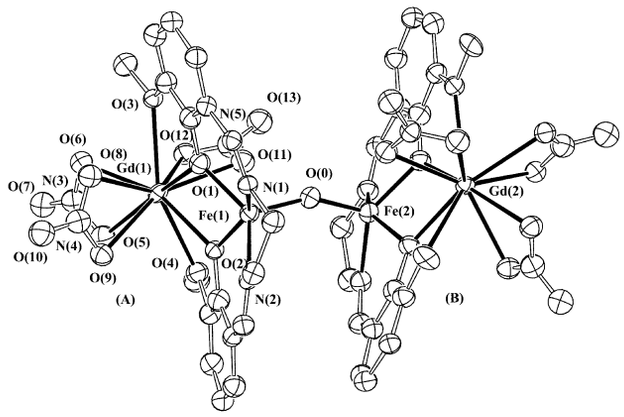

Fig. 1 Zortep view of complex **2** with ellipsoids drawn at the 50% probability level.

pyramidal geometry. Indeed, the key shape-determining angle e_3 defined by Muetterties and Guggenberger[21] is equal to 12.0° for Fe1 and 4.1° for Fe2. A 0° value is expected for e_3 in a perfect square pyramid while a value of 53.1° characterizes a perfect trigonal byramid. The four basal donors (N_2O_2) are afforded by the ligand L while the apical position is occupied by the bridging oxygen, as in the previously published structural determinations of $(Fesalen)_2O$ complexes.[22–24] The structure results from the insertion of a gadolinium ion into each vacant coordination site of the dinuclear ferric complex **1**. A double bridge links the Fe^{III} and Gd^{III} ions *via* the phenolato oxygen atoms. The central Fe–O–Fe unit is marginally affected. Its bending increases slightly (153.1(1)°) in comparison with data related to previously published $(Fesalen)_2O$ complexes (142.4(5)–144.6(6)°)[22–24] while the bridging Fe–O bonds show a mean value of 1.77 Å similar to the one found in $(Fesalen)_2O$ complexes. These Fe–O bonds are significantly shorter than the basal Fe–O bonds which are slightly larger in **2** compared to $(Fesalen)_2O$ (1.94 *vs.* 1.91 Å). On the contrary the equatorial Fe–N bonds are shorter in **2** compared to $(Fesalen)_2O$ (2.04 *vs.* 2.10 Å), while the Fe ··· Fe distance is only slightly larger in **2** compared to $(Fesalen)_2O$ (3.4343(5) *vs.* 3.40 Å).

In the tetranuclear complex **2**, the two gadolinium ions are ten coordinate. Each coordination sphere includes two phenolato oxygen atoms also linked to a ferric ion, two oxygen donors from the methoxy side-arms and six oxygen atoms from three nitrato ions acting as η^2 chelating ligands. The $Fe(O)_2Gd$ units are not strictly planar, the dihedral angle between the Fe(*i*)O(1)O(2) and Gd(*i*)O(1)O(2) planes being equal to 9.9(3)° (*i* = 1) and 14.2(3)° (*i* = 2). This angle varies from 6.2 to 24.1° in the related (Fe^{II}, Gd^{III}) complexes.[15] The $Fe^{III}(i)$ ··· $Gd^{III}(i)$ separations are equal to 3.5189(4) Å (*i* = 1) and 3.5131(4) Å (*i* = 2). They do not significantly differ from the Fe^{II} ··· Gd^{III} distances (3.41–3.52 Å). The Gd–O bond lengths depend on the nature of the oxygen atoms. As usual[8–10] the shortest bonds involve the phenolato oxygen atoms (2.392(2), 2.377(2) Å) and the larger ones involve the methoxy groups (2.676(2), 2.670(2) Å). The shortest intermolecular metal–metal separations are large enough to preclude any interaction (5.6986(4) Å for Fe ··· Gd, 7.6575(4) Å for Gd ··· Gd and 9.5338(8) Å for Fe ··· Fe).

Magnetic study

The magnetic behaviour of μ-oxo diiron(III) complexes is well-documented.[16–18,25,26] The two metal ions are antiferromagnetically coupled with an exchange constant $J \sim 100$ cm^{-1}, the related Hamiltonian being $H = -2JS_{Fe1}S_{Fe2}$. The energy spectrum of these systems comprises a non-magnetic ground state ($E(0)$, $S_T = 0$) and excited states specified by the values of their quantum number (S_T) and energy ($E(S_T)$). For an antiferromagnetic system $E(S_T)$ increases according to the following expression : $E(S_T) = S_T (S_T + 1) |J|$. The large spread in energy is responsible for depopulation of the higher states ($S_T > 3$) even at room temperature. This is the case for **1**. The thermal variation of its $\chi_M T$ product is represented by curve 1 in Fig. 2. At 300 K, $\chi_M T$ is equal to 0.9 cm^3 K mol^{-1} which is

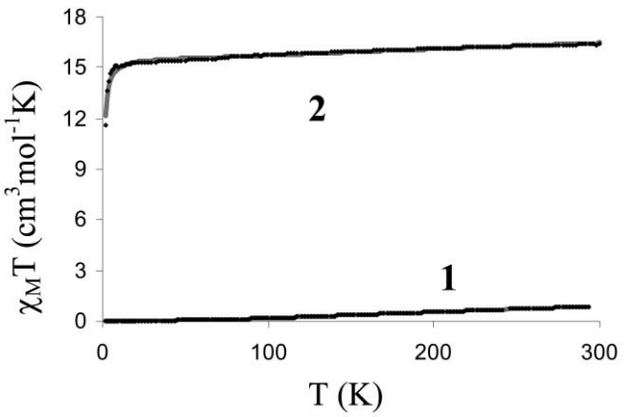

Fig. 2 Thermal dependence of $\chi_M T$ for complexes **1** and **2**. The solid lines represent the best fits of the experimental data.

much smaller than the 8.8 cm^3 K mol^{-1} value expected for two isolated Fe^{III} ions. At 2 K, $\chi_M T$ reaches a small but non zero value (0.01 cm^3 K mol^{-1}) attributable to a small amount (*p*%) of paramagnetic species. This attribution is supported by the presence of a "Curie tail" in the χ_M *vs.* *T* curve. The experimental data are satisfactorily reproduced by the spin cluster model[27] with the parameter values $J = -115.3$ cm^{-1}, $g = 1.90$, $p = 0.14\%$. A more intricate situation prevails for the tetranuclear complex **2**. An appropriate description of its magnetic behaviour requires at least two spin–spin exchange constants related to the (Fe, Fe) and (Fe, Gd) interactions, respectively. These constants are expected to be very different in magnitude (100 *vs.* 0.5 cm^{-1}), and possibly in nature. The thermal dependence of $\chi_M T$ is represented by curve 2 in Fig. 2. $\chi_M T$ decreases from 16.4 (300 K) to 11.8 cm^3 K mol^{-1} (2 K). Both values are smaller than the 23.5 cm^3 K mol^{-1} contribution expected for non interacting spins. Below 25 K, the $\chi_M T$ *vs.* *T* curve shows a steep decrease, the origin of which is questionable. Indeed, such a feature is observed neither for the diiron(III) precursor **1** nor for the previously reported (Fe^{III}, Gd^{III}) and (Fe^{II}, Gd^{III}) complexes. A quantitative analysis was performed within the framework of the spin cluster model[27] with the isotropic Hamiltonian $H = -2[J_{Fe,Fe}S_{Fe1}S_{Fe2} + J_{Fe,Gd}S_{Fe1}S_{Gd1} + J_{Fe,Gd}S_{Fe2}S_{Gd2}]$. To avoid overparametrization it was assumed that the (Fe1, Gd1) and (Fe2, Gd2) interactions are equivalent and that there is no interaction between the terminal Gd1 and Gd2 ions. The fitting process yielded: $J_{Fe,Fe} = -101.4$ cm^{-1}, $J_{Fe,Gd} = -0.7$ cm^{-1}, $g_{Fe} = g_{Gd} = 2.00$ and $p = 0.0\%$. These results support the suggestions of the qualitative examination. The magnitude of the (Fe, Fe) interaction is slightly smaller than for complex **1** but remains within the range of reported values.[17,18] As for (Fe, Gd) interactions, their magnitude ($J = 0.7$ cm^{-1}) compares favourably with the values obtained for known (M, Gd) complexes,[10,15,28,29] but their antiferromagnetic character is rather unexpected: as noted above, most (M, Gd) complexes exhibit a ferromagnetic interaction.[13] Interestingly, modelling of the field dependence of the magnetization supports the presence of an antiferromagnetic (Fe, Gd) interaction (Fig. 3). Indeed, a satisfying agreement is obtained upon comparison of the experimental magnetization values to those calculated with the parameters deduced from the fit of the $\chi_M T$ *vs.* *T* experimental data. It may be noted that *M* saturates for magnetic fields ⩾ *ca.* 4.5 Tesla. The corresponding M_{sat} value of 13.8 BM is attributable to a system with a spin $S_T = 7$ and $g = 1.97$. This result suggests that 4.5 Tesla is a strong enough field to disrupt the (Fe, Gd) coupling but not the much larger (Fe, Fe) interaction

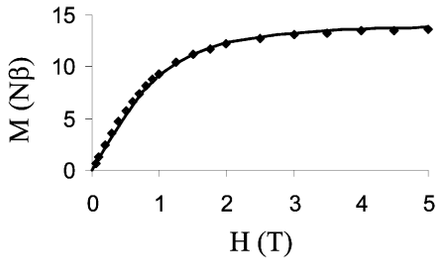

Fig. 3 Field dependence of the magnetization for complex **2** at 2 K. The solid line represents the data computed with the set of parameters obtained from the best fit of the $\chi_M T$ curve shown in Fig. 2 (see text).

with the net result of a high-field magnetism solely attributable to two Gd^{III} ions ($S_{Gd} = 7/2$).

The computational approach used allows access to both the eigenfunctions and energies of the spin system and, in the present case, to compare the situations resulting from a sign reversal of the (Fe, Gd) interactions. The two possibilities, subsequently labeled af–af and af–f, were evaluated with $J_{FeFe} = -101.4$ cm^{-1} and $J_{FeGd} = -$ or $+$ 0.7 cm^{-1}, respectively. In Fig. 4, the energy spectrum of **1**, which as previously noted comprises six levels, is included for comparison with the energy spectrum of **2**. The additional interactions between the Fe^{III} and Gd^{III} ions increase the number of levels from 6 up to 218, but due to the small value of the J_{FeGd}/J_{FeFe} ratio the six multiplets of the energy level scheme of **2** are located at

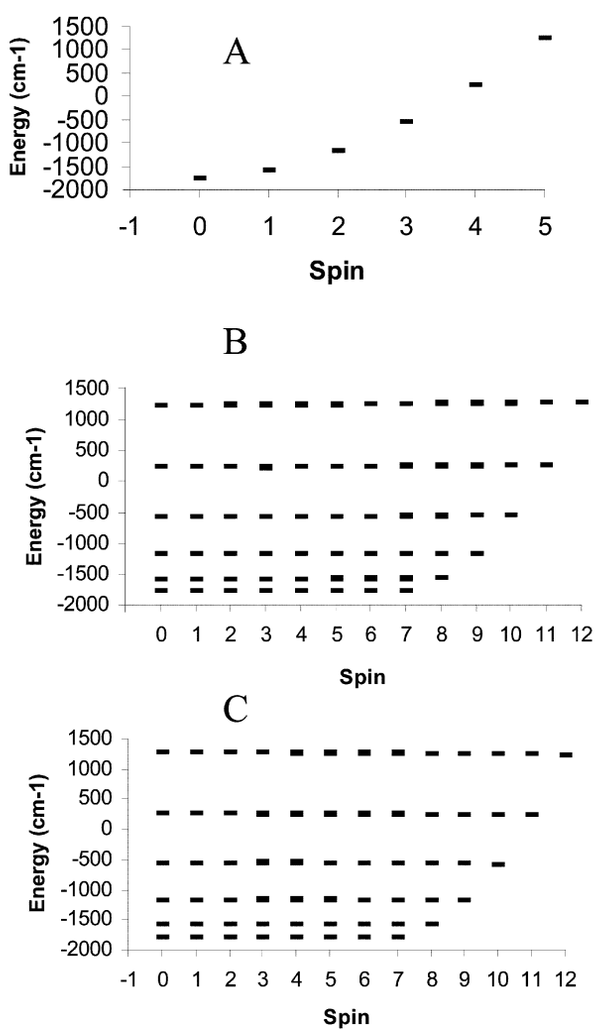

Fig. 4 Energy spectra of complexes **1** (A) and **2** (B, af–af interaction and C, af–f interaction).

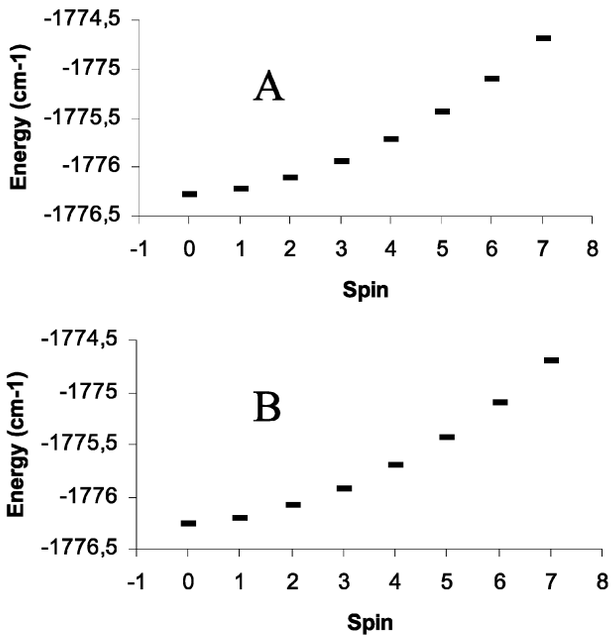

Fig. 5 Enlargement of the two lowest multiplets of complex **2** in the af–f (A) and af–af (B) situations (see text).

positions very close to those for **1**.[27] Within each multiplet, the gaps between the components are very small and prevent any overlap. The two lowest multiplets are enlarged in Fig. 5: independently of the antiferromagnetic or ferromagnetic nature of the (Fe, Gd) interaction, the ground multiplet comprises 8 components with energies ranging from 0 to 1.6 cm^{-1} and spin S_T from 0 to 7, respectively. In both situations the ground level is non-magnetic ($S_T = 0$) but levels with S_T as large as 7 are readily accessible. Differences between the two coupling situations become perceptible for the next multiplets located ≈200 cm^{-1} higher (Fig. 6): they increase with energy, thus favouring the af–af arrangement. Regarding magnetic susceptibility, the two coupling schemes (af–f and af–af) can be differentiated only at high temperature ($T > 100$ K, Fig. 7). The situation would be quite different for the f–f and f–af schemes which

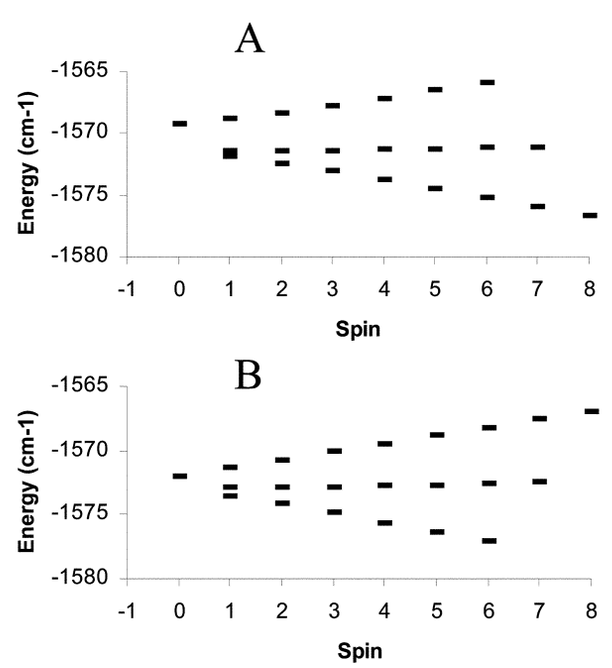

Fig. 6 Enlargement of the two higher multiplets of complex **2** in the af–f (A) and af–af (B) situations (see text).

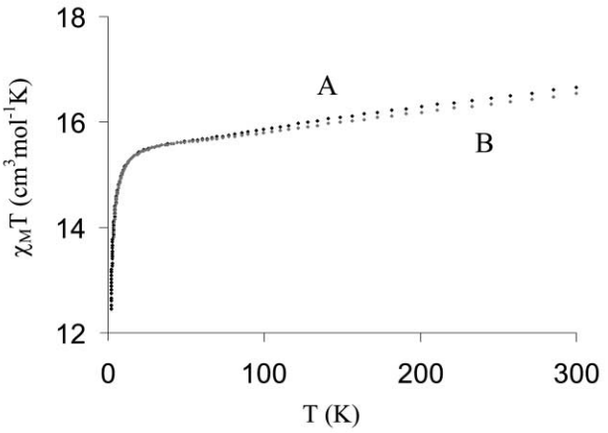

Fig. 7 Theoretical variation of $\chi_M T$ for complex **2** in the two considered situations (A, af–f with $J_{FeFe} = -101.4$ cm^{-1}, $J_{FeGd} = 0.7$ cm^{-1}; B, af–af with $J_{FeFe} = -101.4$ cm^{-1}, $J_{FeGd} = -0.7$ cm^{-1}).

would display distinct ground states ($S_T = 12$ and $S_T = 2$ respectively).

Finally, the experimental study of the bulk magnetic properties of **2** and the related theoretical modelling should afford convergent support to the presence of ferromagnetic or antiferromagnetic (Fe^{III}, Gd^{III}) interactions. Unfortunately the value of this parameter is too weak, compared to the strong Fe–Fe interaction. As a result, the difference between the two situations in Fig. 7 is in the range of the experimental error on the measurement. Although the theoretical modelling better agrees with an antiferromagnetic interaction, $J_{Fe,Gd} = -0.7$ cm^{-1}, this negative value can not be unequivocally confirmed. Nevertheless this result contrasts with our previous finding of ferromagnetic interactions in dinuclear (Fe^{III}, Gd^{III}) and (Fe^{II}, Gd^{III}) complexes but we must keep in mind that antiferromagnetic (M, Gd) interactions do not correspond to a completely unusual phenomenon. Furthermore it may be noted that the (Fe, Fe) coupling is affected by the addition of the gadolinium ions; its magnitude decreases from 115.3 cm^{-1} in **1** to 101.4 cm^{-1} in **2**.

Experimental

Materials and methods

All starting materials were purchased from Aldrich and used without further purification. LH_2[30] was obtained as previously described.

$(LFe)_2O\cdot(CH_2Cl_2)$ 1. To a suspension of LH_2 (1.32 g, 4×10^{-3} mol) in methanol (50 mL) was first added $FeCl_3$ (0.65 g, 4×10^{-3} mol) in methanol (10 mL) and then triethylamine (1 mL). The mixture was stirred and gently heated for 20 minutes, yielding an orange precipitate which was filtered off and washed with a minimum amount of cold methanol. The powder was reprecipitated from CH_2Cl_2. Anal. Calc. for $C_{37}H_{38}Cl_2Fe_2N_4O_9$: C, 51.4; H, 4.4; N, 6.5. Found: C, 51.3; H, 4.4; N, 6.4%. Characteristic IR absorptions (KBr, cm^{-1}): 1621 s, $\nu_{C=N}$, 841 m, ν_{FeOFe}.

$\{[LFeGd(NO_3)_3]_2O\}(CH_3COCH_3)$ 2. A slight excess of $Gd(NO_3)_3\cdot 6H_2O$ (0.32 g, 7×10^{-4} mol) was added to a suspension of $(LFe)_2O\cdot(CH_2Cl_2)$ (0.43 g, 5×10^{-4} mol) in acetone (15 mL) at room temperature. Stirring induced a quick dissolution and, several minutes later, precipitation of a maroon powder which was filtered off two hours later, and washed with acetone and diethyl oxide. Yield: 0.6 g (80%). Anal. Calc. for $C_{39}H_{42}Fe_2Gd_2N_{10}O_{28}$: C, 30.7; H, 2.8; N, 9.2. Found: C, 30.5; H, 2.7; N, 9.0%. Characteristic IR absorptions (KBr, cm^{-1}): 1712 m, $\nu_{C=O}$; 1621 s, $\nu_{C=N}$; 1471 s, 1282 s, ν_{NO_3}, 887 m, ν_{FeOFe}.

Table 1 Crystal data and structure refinement for $\{[LFeGd(NO_3)_3]_2O\}(CH_3COCH_3)$

Formula	$C_{39}H_{42}Gd_2Fe_2N_{10}O_{28}$
M	1525.03
Crystal dimensions/mm	0.40 × 0.20 × 0.15
Crystal system	Monoclinic
Space group	$P2_1/n$ (no. 14)
a/Å	15.346(2)
b/Å	17.3716(16)
c/Å	19.625(2)
β/°	100.589(14)
V/Å^3	5142.7(10)
Z	4
F(000)	3000
T/K	140
D_c/Mg m^{-3}	1.970
μ(Mo-Kα)/mm^{-1}	3.201
No. collected reflections	40916
No. unique reflections	8134 [$R_{int} = 0.0346$]
No. of observed reflections	6713
No. of refined parameters	730
$wR(F^2)$	0.0572
$R[F>4\sigma(F)]$	0.0280
Goodness of fit on F^2	1.035
($\Delta\rho$) max, min/e Å^{-3}	1.298, −0.839

Crystallographic data collection and structure determination for 2

The crystallographic data together with the refinement details for $\{[LFeGd(NO_3)_3]_2O\}(CH_3COCH_3)$ are summarized in Table 1. Some selected lengths, distances and angles are given in Table 2. The selected crystal of **2** (red plate, 0.40 × 0.20 × 0.15 mm) was mounted on a Stoe Imaging Plate Diffractometer System (IPDS) equipped with an Oxford Cryosystems cooler device at 140 K using a graphite monochromator ($\lambda = 0.71073$ Å). The crystal-to-detector distance was 80 mm (max θ value 24.17°). Data were collected[31] with a φ rotation movement ($\varphi = 0.0$–250.5°, $\Delta\varphi = 1.5$°). 40916 reflections were collected, of which 8134 independent ($R_{int} = 0.0346$). Numerical absorption[32] corrections were applied. Maximum and minimum transmission factors were respectively 0.7161 and 0.4317. The structure was solved by direct methods using SHELXS-97[33] and refined by full-matrix least-squares on F_o^2 with SHELXL-97[34] with anisotropic displacement parameters for all non-hydrogen atoms. H atoms were introduced in calculations using the riding model with isotropic thermal parameters 1.1 times higher than those of the riding atom. Scattering factors were taken from ref. 35. The molecular plot was obtained using the ZORTEP program.[36]

CCDC reference number 197093.

See http://www.rsc.org/suppdata/dt/b2/b210950f/ for crystallographic data in CIF or other electronic format.

Physical measurements

Elemental analyses were carried out at the Laboratoire de Chimie de Coordination Microanalytical Laboratory in Toulouse, France, for C, H, and N. IR spectra were recorded on a GX system 2000 Perkin-Elmer spectrophotometer. Samples were run as KBr pellets. Mössbauer measurements were obtained as previously described.[15] Magnetic data were obtained with a Quantum Design MPMS SQUID susceptometer. Magnetic susceptibility measurements were performed in the 2–300 K temperature range in a 0.8 T applied magnetic field, and diamagnetic corrections were applied by using Pascal's constants.[37] Isothermal magnetization measurements as a function of the external magnetic field were performed up to 5 T at 2 K. The magnetic susceptibility has been computed by exact calculation of the energy levels associated to the spin Hamiltonian through diagonalization of the full matrix with a general program for axial symmetry,[38] and with the MAG-

Table 2 Selected bond lengths (Å), distances (Å) and angles (°) for complex **2**

Fe–O(0)	1.763(2)–1.768(2)	Fe(1)–O(0)–Fe(2)	153.1(1)
$Fe–O(1)_{phenolato}$	1.934(2)–1.947(2)	Gd(1)–O(1)–Fe(1)	108.42(8)
$Fe–O(2)_{phenolato}$	1.931(2)–1.934(2)	Gd(2)–O(1)–Fe(2)	106.34(8)
Fe–N(1)	2.037(2)–2.033(2)	Gd(1)–O(2)–Fe(1)	108.36(7)
Fe–N(2)	2.054(2)–2.042(2)	Gd(2)–O(2)–Fe(2)	108.72(8)
$Gd–O(1)_{phenolato}$	2.392(2)–2.428(2)	O(1)–Fe(1)–O(2)	79.71(7)
$Gd–O(2)_{phenolato}$	2.396(2)–2.377(2)	O(1)–Fe(2)–O(2)	79.99(8)
$Gd–O(3)_{methoxy}$	2.551(2)–2.712(2)	O(1)–Gd(1)–O(2)	62.32(6)
$Gd–O(4)_{methoxy}$	2.676(2)–2.670(2)	O(1)–Gd(2)–O(2)	62.53(6)
$Gd–O_{nitrato}$	2.382(2)–2.542(2)	α^a (i = 1)	9.9(3)
Fe(1) ··· Fe(2)	3.4343(5)	α^a (i = 2)	14.2(3)
Gd ··· Fe	3.5189(4)–3.5131(4)		

[a] Dihedral angle between the O–Gd–O and O–Fe–O planes of the bridging network (see text).

PACK program package[27,39] in the case of magnetization. Least-squares fittings were accomplished with an adapted version of the function-minimization program MINUIT.[40]

References

1 C. Benelli, A. Caneschi, D. Gatteschi, J. Laugier and P. Rey, *Angew. Chem., Int. Ed. Engl.*, 1987, **26**, 913–915.
2 C. Benelli, A. Caneschi, D. Gatteschi and L. Pardi, *Inorg. Chem.*, 1992, **31**, 741–746.
3 J. P. Sutter, M. L. Kahn, S. Golhen, L. Ouahab and O. Kahn, *Chem. Eur. J.*, 1998, **4**, 571–576.
4 A. Bencini, C. Benelli, A. Caneschi, R. L. Carlin, A. Dei and D. Gatteschi, *J. Am. Chem. Soc.*, 1985, **107**, 8128–8136.
5 C. Benelli, A. J. Blake, P. E. Y. Milne, J. M. Rawson and R. E. P. Winpenny, *Chem. Eur. J.*, 1995, **1**, 614–618.
6 M. Andruh, I. Ramade, E. Codjovi, O. Guillou, O. Kahn and J. C. Trombe, *J. Am. Chem. Soc.*, 1993, **115**, 1822–1829.
7 I. Ramade, O. Kahn, Y. Jeannin and F. Robert, *Inorg. Chem.*, 1997, **36**, 930.
8 J. P. Costes, F. Dahan, A. Dupuis and J. P. Laurent, *Inorg. Chem.*, 1997, **36**, 3429.
9 J. P. Costes, F. Dahan, A. Dupuis and J. P. Laurent, *Inorg. Chem.*, 1997, **36**, 4284.
10 J. P. Costes, A. Dupuis and J. P. Laurent, *Eur. J. Inorg. Chem.*, 1998, 1543.
11 C. Lescop, D. Luneau, E. Belorisky, P. Fries, M. Guillot and P. Rey, *Inorg. Chem.*, 1999, **38**, 5472–5473.
12 A. Caneschi, A. Dei, D. Gatteschi, L. Sorace and K. Vostrikova, *Angew. Chem., Int. Ed. Engl.*, 2000, **39**, 246–248.
13 J. P. Costes, F. Dahan, A. Dupuis and J. P. Laurent, *Inorg. Chem.*, 2000, **39**, 5994 and references therein.
14 J. P. Costes, F. Dahan, B. Donnadieu, J. Garcia-Tojal and J. P. Laurent, *Eur. J. Inorg. Chem.*, 2001, 363.
15 J. P. Costes, F. Dahan, F. Dumestre, J. P. Tuchagues and J. M. Clemente-Juan, *Inorg. Chem.*, 2001, **41**, 2886.
16 P. Gomez-Romero, E. H. Witten, W. M. Reiff, G. Backes, J. Sanders-Loehr and G. B. Jameson, *J. Am. Chem. Soc.*, 1989, **111**, 9039.
17 K. S. Murray, *Coord. Chem. Rev.*, 1974, **12**, 1.
18 R. N. Mukherjee, T. D. P. Stack and R. H. Holm, *J. Am. Chem. Soc.*, 1988, **110**, 1850.
19 C.-M. Che, C.-W. Chan, S.-M. Yang, C.-X. Guo, C.-Y Lee and S.-M. Peng, *J. Chem. Soc., Dalton Trans.*, 1995, 2961.
20 C. Stockheim, L. Hoster, T. Weyhermüller, K. Wieghardt and B. Nuber, *J. Chem. Soc., Dalton Trans.*, 1996, 4409.
21 E. L. Muetterties and L. J. Guggenberger, *J. Am. Chem. Soc.*, 1974, **96**, 1748.
22 M. Gerloch, E. D. McKenzie and A. D. C. Towl, *J. Chem. Soc. A*, 1969, 2850.
23 P. Coggon, A. T. McPhail, F. E. Mabbs and V. N. McLachlan, *J. Chem. Soc. A*, 1971, 1014.
24 L. O. Atovmyan, O. A. D'yachenko and S. V. Soboleva, *J. Struct. Chem. (USSR)*, 1970, **11**, 517.
25 R. Hotzelmann, K. Wiegardt, U. Flörke, H.-J. Haupt, D. C. Weatherburn, J. Bonvoisin, G. Blondin and J.-J. Girerd, *J. Am. Chem. Soc.*, 1992, **114**, 1681.
26 T. Jüstel, M. Müller, T. Weyhermüller, C. Kressl, E. Bill, P. Hildebrandt, M. Lengen, M. Grodzicki, A. X. Trautwein, B. Nuber and K. Wiegardt, *Chem. Eur. J.*, 1999, **2**, 793.
27 J. J. Borras-Almenar, J. M. Clemente-Juan, E. Coronado and B. S. Tsukerblat, *Inorg. Chem.*, 1999, **38**, 6081.
28 J. P. Costes, F. Dahan, A. Dupuis and J. P. Laurent, *C. R. Acad. Sci. Paris, Ser. IIc*, 1998, **1**, 417.
29 J. P. Costes, F. Dahan and J. Garcia-Tojal, *Chem. Eur. J.*, 2002, in press.
30 P. Guerriero, S. Tamburini, P. A. Vigato, U. Russo and C. Benelli, *Inorg. Chim. Acta*, 1993, **213**, 279.
31 STOE, IPDS Manual. Version 2.93. Stoe & Cie, Darmstadt, Germany, 1997.
32 Stoe, X-SHAPE. Crystal Optimisation for Numerical Absorption Corrections, Revision 1.01. Stoe & Cie, Darmstadt, Germany, 1996.
33 G. M. Sheldrick, SHELXS-97. Program for Crystal Structure Solution, University of Göttingen, Göttingen, Germany, 1990.
34 G. M. Sheldrick, SHELXL-97. Program for the refinement of crystal structures from, diffraction data, University of Göttingen, Göttingen, Germany, 1997.
35 *International Tables for Crystallography*, Kluwer Academic Publishers, Dordrecht, The Netherlands, 1992, Vol. C.
36 L. Zsolnai, H. Pritzkow, G. Huttner, ZORTEP. Ortep for PC, Program for Molecular Graphics, University of Heidelberg, Heidelberg, Germany, 1996.
37 P. Pascal, *Ann. Chim. Phys.*, 1910, **19**, 5.
38 J. M. Clemente-Juan, C. Mackiewicz, M. Verelst, F. Dahan, A. Bousseksou, Y. Sanakis and J.-P. Tuchagues, *Inorg. Chem.*, 2002, **41**, 1478.
39 J. J. Borrás-Almenar, J. M. Clemente-Juan, E. Coronado and B. S. Tsukerblat, *J. Comput. Chem.*, 2001, **22**, 985.
40 F. James and M. Roos, MINUIT Program, a System for Function Minimization and Analysis of the Parameters Errors and Correlations, *Comput. Phys. Commun.*, 1975, **10**, 345.